

Intrinsic Photoconductivity of Ultracold Fermions in Optical Lattices

J. Heinze,^{*} J. S. Krauser,^{*} N. Fläschner,^{*} B. Hundt, S. Götze, K. Sengstock,[†] and C. Becker
Institut für Laser-Physik, Universität Hamburg, Luruper Chaussee 149, 22761 Hamburg, Germany

We report on the first experimental observation of a persistent alternating photocurrent in an ultracold gas of fermionic atoms in an optical lattice. The dynamics is induced and sustained by an external harmonic confinement. We find a counterintuitively momentum-dependent oscillation frequency for excited particles and a fast decay of holes which we attribute to spatial trapping. Lifetime measurements reveal a significant enhancement of particle-hole recombination with increasing interactions.

PACS numbers: 37.10.Jk, 78.56.-a, 72.20.Jv, 03.75.Ss

Photoconductivity describes the change of a materials conductivity following an excitation with incident photons. If the photon energy is resonant with a band transition, electrons are excited from the valence band to the conduction band and an initial insulator becomes conducting [1]. Today, photoconductivity is widely used in technological applications such as semiconductor photodiodes and photoresistors. It also provides a powerful probe for novel materials, such as graphene [2], transistors made from carbon nanotubes [3] or semiconductor nanowires [4]. To extend the understanding of such complex materials, atomic quantum gases have proven to be powerful model systems. In this context, however, it is desirable to develop and adopt versatile probing methods [5–7]. Owing to its excitational structure in several bands, photoconductivity can provide deeper insight into intra- and interband dynamics as well as orbital effects, which gained much interest in recent years. In the field of quantum gases, multiband interactions and dynamics have been experimentally studied mainly with bosonic atoms [8–17]. For fermionic atoms, population transfers into higher bands have been recently demonstrated via Landau-Zener transitions across Dirac cones [18] and momentum-resolved lattice amplitude modulation [19].

In this letter, we study experimentally and theoretically the photoconductivity of fermionic atoms in an optical lattice. We create uncoupled particle and hole excitations using lattice amplitude modulation and thoroughly investigate the dynamics of the atoms in the second excited band as well as the holes in the valence band. The lattice modulation corresponds to the incident photons in solid state photoconductivity experiments, while the atoms (holes) correspond to the electrons (holes) in the conduction (valence) band. A typical difference between ultracold gas experiments and real materials is the presence of an overall harmonic confinement, which - in our experiment - plays the role of an external force. It induces pronounced oscillations of the atoms in the excited band with a counterintuitive dispersion relation which differs maximally from the zero lattice case for shallow lattices. We explain this with a reduced effective mass in the conduction band. In strong contrast to the long-lived coherent dynamics of the atoms, we observe a dramati-

cally shorter lifetime of the holes in the valence band. We attribute this effect - generic to harmonically trapped lattice systems - to spatial trapping at localized states at the edge of the atomic cloud. As a key result of this paper, photoconduction of fermionic atoms is mainly connected to long-lived populations in excited bands, forming the majority component, whereas holes in the valence band decay quickly.

For the experiments we prepare either a spin-polarized Fermi gas with $m = 9/2$ or an interacting binary spin mixture of $m = -9/2$ and $m = -5/2$ in the $f = 9/2$ groundstate manifold of ^{40}K (for details see [20]). The atoms are held in the combined potential of an optical dipole trap with variable trapping frequency ω_0 and an optical lattice at $\lambda = 1030\text{ nm}$. To induce a photocurrent, we excite the system via lattice modulation spectroscopy [21, 22] as explained in [19]. This two-photon process creates particle excitations in the conduction band and leaves vacancies (holes) in the valence band. Both have the same initial quasimomentum q_0 . Due to the different curvature of the involved bands, q_0 can be arbitrarily tuned by choosing a particular modulation frequency [see Fig. 1(a)]. To record the time evolution of the excited system, we detect the quasimomentum distribution by performing adiabatic bandmapping followed by resonant absorption-imaging after 15 ms time-of-flight [19, 23]. Recall, that the bandmapping technique maps particles in the second excited band to real momenta in the interval $k/k_{\text{BZ}} = [2, 3]$ and $k/k_{\text{BZ}} = [-3, -2]$, constituting the third Brillouin zone. Particles in the lowest band are mapped to $k/k_{\text{BZ}} = [-1, 1]$, with $k_{\text{BZ}} = 2\pi/\lambda$.

A typical time evolution for a spin-polarized gas is shown in Fig. 1(b) after an excitation at a quasimomentum $q_0 = 0.5$ and a lattice depth of $s = 10$ in units of the recoil energy $E_r = \hbar^2 k_{\text{BZ}}^2 / 2m$ with m the mass of ^{40}K . The atoms in the conduction band show a pronounced oscillation in momentum space. The decay time of the excitations is of the order of 100 ms. This indicates a very slow recombination between particles and holes. However, the holes in the valence band undergo a fast decay and are only visible in momentum space for the first 2 ms. This indicates a local trapping of the holes within the valence band, reminiscent of trapping of charge car-

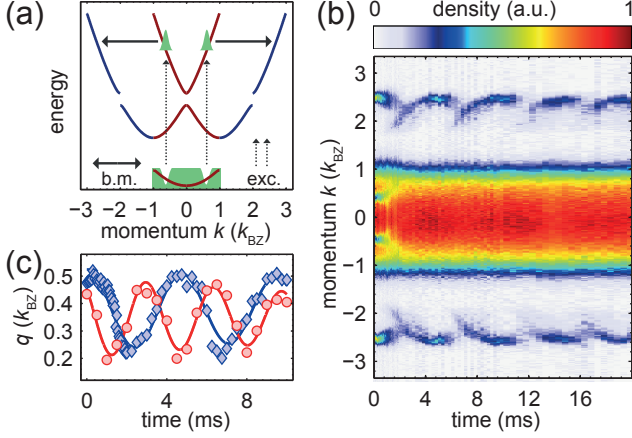


FIG. 1. (a) Principle of excitation via lattice amplitude modulation (dotted lines) and band mapping process (solid lines) in momentum space. (b) Measured photocurrent after excitation to the conduction band at $10E_r$. Shown are the column densities of the momentum distribution at different times after the excitation. Atoms in the valence band are represented by the central plateau. The excitations in the conduction band clearly oscillate in momentum space. (c) Center-of-mass quasimomentum of the particle-excitation in the conduction band at $10E_r$ for two different trapping frequencies $\omega_0 = 2\pi \times 66$ Hz (circles) and $\omega_0 = 2\pi \times 50$ Hz (diamonds). Solid lines are fits to the data. Extracted oscillation frequencies are $\Omega = 2\pi \times 295 \pm 9$ Hz (circles) and $\Omega = 2\pi \times 213 \pm 3$ Hz (diamonds).

riers in photoconducting solids [1]. Consequently, the excited atoms form the majority component of the photocurrent in our system. We concentrate on their behavior in the following and afterwards analyze the trapping of the holes in more detail. Our method is related to the measurements in [13] using bosonic atoms, where oscillations in the spatial domain were studied. Hence, neither holes nor excitations with small q_0 could be investigated.

We first examine the effect of the harmonic trapping potential on the dynamics of the particles. Figure 1(c) shows two typical measurements with different harmonic trapping frequencies ω_0 for otherwise equal initial parameters. Fits to the data reveal, that the oscillation frequency linearly depends on ω_0 but is substantially higher than the bare trapping frequency. This result significantly deviates from the dynamics in harmonic potentials without any lattice, where the oscillation frequency is equal to ω_0 . To understand the main features of the photocurrent we first present two simplified descriptions before we describe the complete experimental and numerical results.

Consider the case of a particle at a given quasimomentum in an excited band of an optical lattice. This is depicted in Fig. 2(a) using the extended zone scheme. In the presence of an harmonic confinement different quasimomenta are coupled which causes an oscillation in momentum space. The existence of a substantial band gap

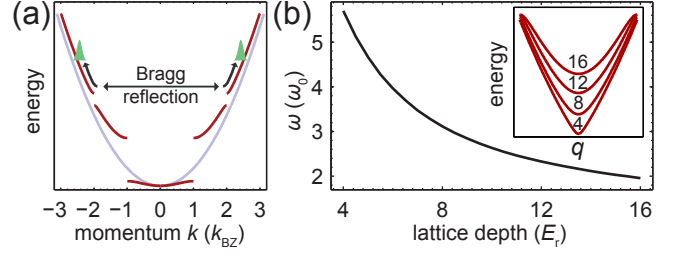


FIG. 2. (a) Sketch of the time evolution of atoms in the conduction band using the extended zone scheme. (b) Oscillation frequency in the conduction band at $q_0 = 0$ for different lattice depths, calculated with (1). Inset shows the complete conduction band for 4, 8, 12 and 16 E_r . Note the decrease in curvature with increasing lattice depth, leading to an increase of the effective mass m' .

between first and second excited band leads to a striking modification of the simple harmonic oscillator dynamics: When a particle with initial quasimomentum q_0 reaches the gap, it is Bragg reflected and thus omits a huge part of the extended zone scheme. The oscillation continues until the particle reaches $-q_0$ and is reversed. Thus, depending on q_0 , the intraband dynamics is limited to different fractions of the harmonic oscillation. This leads to a strong momentum dependence of the oscillation frequency $\omega(q_0)$. In summary, by omitting the inner part of the spectrum, the oscillation period is dramatically decreased in comparison to the pure harmonic case. Recall that the oscillation is still driven by the harmonic trap and thus the frequency is proportional to ω_0 as observed experimentally.

For oscillations with small initial quasimomentum, there is a complementary explanation which exploits the form of the bands in the reduced zone scheme. It shows, that the photocurrent frequency non-trivially depends on the lattice depth: The presence of an optical lattice results in a modified kinetic energy with a momentum-dependent effective mass. Around $q = 0$, where the conduction band has a minimum, this effective kinetic energy can be approximated as a quadratic dispersion with a renormalized mass m' . The effective Hamiltonian is thus given by

$$H = \frac{p^2}{2m'} + \frac{1}{2}m\omega_0^2 x^2 = \frac{p^2}{2m'} + \frac{1}{2}m'\omega^2 x^2, \quad (1)$$

where m is the real mass of the particles and $\omega = \sqrt{m/m'}\omega_0$ the renormalized trapping frequency. Especially for shallow lattices the effective mass m' becomes much smaller than m and thus ω becomes very large, as shown in Fig. 2(b). This result leads to the counterintuitive feature, that the dynamics in shallow lattices maximally differs from the zero lattice case. This apparent contradiction is resolved by the onset of Landau-Zener tunneling to the first excited band in very shallow lat-

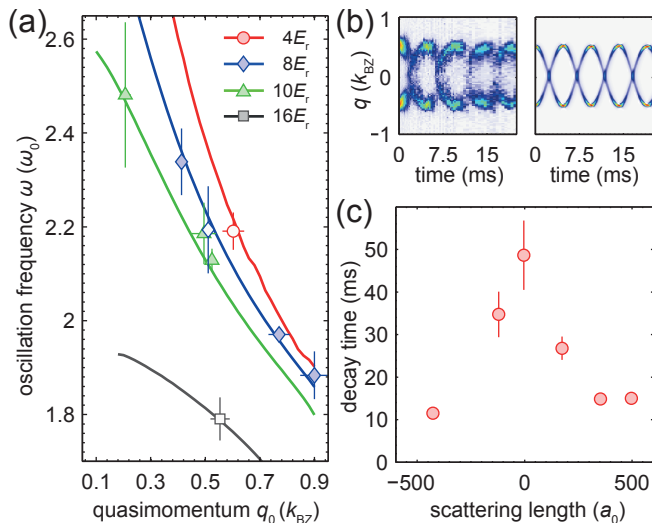


FIG. 3. (a) Comparison of measured frequencies and numerical results for different lattice depth and quasi-momenta. Filled symbols represent measurements with non-interacting mixtures. Open symbols show data with interacting mixtures. Lines show numerical calculations using the full trapping and lattice potential. Note the strong increase of ω for shallow lattices and small q . (b) Exemplary comparison of experimental data (left) and numerical result (right) for the time evolution in the conduction band. Only the third Brillouin zone is depicted. (c) Decay time of particles from the conduction band as a function of the scattering length for a 3D lattice of $8E_F$. Shown is the time after the excitation until only $1/e$ atoms are still in the conduction band. All error bars solely correspond to fit errors, representing two standard deviations.

tices. The bandgap becomes small and vanishes in the zero-lattice limit, where the atoms oscillate in the harmonic confinement with the bare trapping frequency ω_0 . In contrast to the conduction band, in the valence band the effective mass m' is always larger than m for any lattice depth and thus the oscillation frequency is smaller than ω_0 . Therefore, photoconductivity in the conduction band qualitatively differs from the conduction in the valence band.

We measured the photocurrent in our system to investigate all abovementioned dependencies. Figure 3(a) shows our measurements of the photocurrent frequency as a function of the lattice depth and the initial quasimomentum. For spin-polarized gases, we measured the frequency of the conduction band photocurrent at $s = 8$ and $s = 10$ for different q_0 . In the interacting case we investigated the three lattice depths $s = 4, 8, 16$ at the background scattering length of $168.5 a_0$ [24]. All data exhibit the behavior expected from the argumentation presented in connection to Fig. 2: The oscillation frequency ω decreases with increasing lattice depth and increasing q_0 .

To obtain a quantitative prediction for the dispersion relation $\omega(q_0, s)$ of the photocurrent, we performed nu-

merical calculations. We assume a single particle in the conduction band, represented by a Gaussian distribution of Bloch states centered around a given quasimomentum q_0 . This state is subject to the full potential of the optical lattice and the harmonic confinement. For further details see [20]. The results of our calculation are presented in Fig. 3(a) in comparison with our experimental data, showing very good agreement. Figure 3(b) displays an exemplary comparison of experimental data in momentum space and a corresponding calculation. The oscillatory behavior with a renormalized frequency is clearly reproduced by the numerical results. In particular, the calculations confirm the experimentally determined linear dependence between ω and the bare trapping frequency ω_0 for all q_0 . Moreover, we find that for small q_0 , where (1) is valid, it agrees with the numerical results.

For the interacting case, no significant deviations from the single-particle picture could be observed in the oscillation frequency. In contrast to the spin-polarized case, however, we find a substantially enhanced decay rate of atoms from the conduction band. This includes both, loss of particles from the trap and decay of particles into lower bands. To investigate the decay-dependence on the interaction strength, we used a Feshbach resonance at 224 G [25] with a width of 7.6 G [26]. The corresponding data is shown in Fig. 3(c). The total decay rate from the conduction band strongly depends on the interaction, while the total atom loss is independent of the scattering length, which we checked independently. Thus, the results are a measure for the time needed for recombination of free charge carriers, which increases with decreasing interaction as naively expected and shows a maximum at vanishing interaction. As an application, this effect might be used as a new probe to characterize more precisely the zero-crossing of Feshbach resonances. In conclusion, we find very good agreement of experiment and numerical calculations for many different parameters, which shows, that photoconductivity of excited fermions in optical lattice with superimposed harmonic traps can be thoroughly understood.

In addition to the excited particles in the conduction band, one can clearly observe holes in the valence band in the photoconduction measurement of Fig. 1(b). As shown in more detail in Fig. 4(a), the holes decay, however, very fast on the timescale of a few ms, which cannot be explained by recombination with excited atoms, which have a much longer lifetime [see Fig. 3(c)]. The decay of the holes in momentum space instead indicates spatial trapping, which is also observed in photoconducting normal insulators [1]. In these systems, local imperfections of the periodic potential typically lead to trapping of the holes, which can no longer participate in the photocurrent anymore. In ultracold atom experiments, it is well known, that the harmonic potential leads to localized states at the edge of the system [27]. These states are off-resonant for tunneling in the lattice, since the lo-

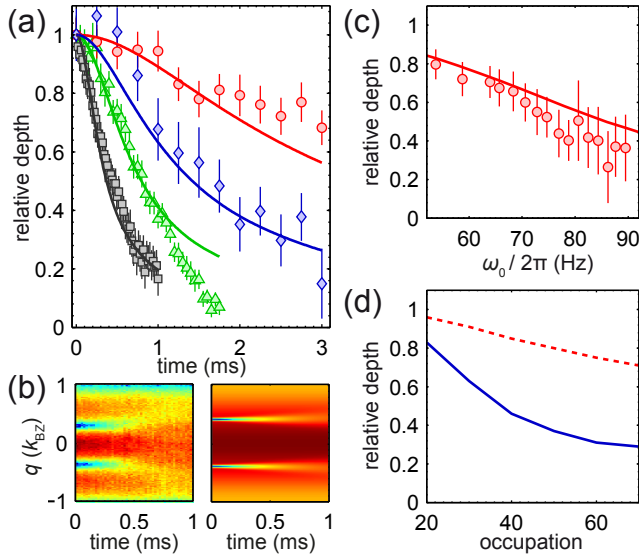


FIG. 4. (a) Time evolution of relative hole depth for different configurations. Circles: $4 E_r$, $q_0 = 0.0$, $\omega_0 = 20$ Hz, interacting mixture; Diamonds: $4 E_r$, $q_0 = 0.0$, $\omega_0 = 36$ Hz, interacting mixture; Triangles: $10 E_r$, $q_0 = 0.5$, $\omega_0 = 50$ Hz; Squares: $6 E_r$, $q_0 = 0.4$, $\omega_0 = 63$ Hz. Solid lines are single-particle calculations as described in the text. (b) Exemplary comparison of experimental data (left) and numerical result (right) for the time evolution in the valence band. Only the first Brillouin zone is depicted. (c) Relative hole depth after $250 \mu s$ for different trapping frequencies at $4 E_r$, $q_0 = 0.5$ in an interacting mixture. Solid line is a single-particle calculation with an occupation of 40 states in the lattice direction. All error bars solely correspond to fit errors, representing two standard deviations. (d) Numerical results for the relative hole depth as in (c) for $\omega_0 = 2\pi \times 50$ Hz (dashed) and $2\pi \times 90$ Hz (solid) as a function of the number of occupied states in the lattice direction.

cal potential difference between two neighboring sites is larger than the bandwidth of the lattice. This is true both for particles and for holes. However, for a hole to be dynamically trapped in localized states, in analogy to real solids, it is necessary, that these state are occupied by particles before the excitation. Since the localized states are at the edge of the atomic cloud, their occupation increases with the filling and the lifetime of the holes should decrease accordingly.

To quantitatively analyze the trapping of the holes in our experiment, we adopt a theoretical description from solid state physics, where holes in an otherwise completely filled valence band can be described as particles with negative mass. We have simulated the holes in analogy to the excited particles by assuming a single particle with negative mass in the valence band of the combined periodic and harmonic potential (see [20] for details). Figure 4(a) shows, that the decay of the holes can be very accurately described by our model for various regimes. Exemplarily, in Fig. 4(b) a comparison of experimental and numerical data in momentum space shows

the fast decay of a hole in less than 1 ms.

As for the excited atoms in the conduction band, we investigated the influence of the harmonic trapping in detail. Figure 4(c) shows the decay of a hole in dependence of ω_0 . The lifetime of the holes clearly decreases with increasing ω_0 in good agreement with our numerical calculations. The main effect of the increased confinement is to increase the local potential difference between two neighboring sites. This creates more localized states near the center of the system. At constant total filling, the result is a higher relative population of such localized states. Assuming local trapping of the holes, this explains the decrease in lifetime. We also numerically checked the dependence on the filling at constant trapping strength. The results are shown in Fig. 4(d) for two different trapping frequencies ω_0 . At high filling the holes decay much faster than for a system with low filling. This supports our experimental findings from Fig. 4(c) and our intuitive explanation.

In conclusion we have presented a comprehensive study of photoconductivity in an ultracold gas of fermionic atoms. By independently analyzing the dynamics of excited particles and holes we have shown that atoms in the conduction band constitute the majority charge carriers in our system. The observed long-lived oscillatory dynamics could be reproduced very well by our numerical simulations and proves to be very sensitive to the harmonic as well as the lattice potential. In particular we measure that counterintuitively the dynamics maximally differs from the purely harmonically trapped case in very shallow lattices. Opposed to the persistent dynamics of the atoms in the excited band, we observe a very short free-carrier lifetime of the holes which we attribute to trapping in localized states at the edge of the combined lattice and harmonic potential. These results may prove crucial for further studies on particle-hole excitations such as excitons. The presented measurements extend the available techniques to explore dynamical properties of optical lattice systems and equally important emphasize the increased role of the harmonic confinement for experiments involving excited spatial bands. Finally, our results constitute an important contribution for the understanding of fundamental dynamical properties of fermionic quantum gases in optical lattices.

We thank P. Törmä for valuable discussion. We acknowledge financial support by DFG via Grant No. FOR801.

* J. Heinze, J. S. Krauser and N. Fläschner contributed equally to this work.

† Corresponding author: klaus.sengstock@physnet.uni-hamburg.de

[1] R. H. Bube, Photoconductivity in solids, John Wiley and Sons (1960)

- [2] E. J. H. Lee, K. Balasubramanian, R. T. Weitz1, M. Burghard, and K. Kern, *Nature Nano.* **3**, 486 (2008)
- [3] M. Freitag, J. C. Tsang, A. Bol, D. Yuan, J. Liu, and P. Avouris, *Nano Lett.* **7**, 2037 (2007)
- [4] Y. Ahn, J. Dunning, and J. Park, *Nano Lett.* **5**, 1367 (2005)
- [5] D. Jaksch, C. Bruder, J. I. Cirac, C. W. Gardiner, and P. Zoller, *Phys. Rev. Lett.* **81**, 3108 (1998)
- [6] M. Lewenstein, A. Sanpera, V. Ahufinger, B. Damski, A. Sen and U. Sen, *Adv. Phys.* **56**, 243 (2007).
- [7] I. Bloch, J. Dalibard, and W. Zwerger, *Rev. Mod. Phys.* **80**, 885 (2008)
- [8] E. Peik, M. B. Dahan, I. Bouchoule, Y. Castin, and C. Salomon, *Phys. Rev. A* **55**, 2989 (1997)
- [9] T. Salger, C. Geckeler, S. Kling, and M. Weitz, *Phys. Rev. Lett.* **99**, 190405 (2007)
- [10] T. Müller, S. Fölling, A. Widera, and I. Bloch, *Phys. Rev. Lett.* **99**, 200405 (2007)
- [11] D. Clément, N. Fabbri, L. Fallani, C. Fort and M. Inguscio, *New. J. Phys.* **11**, 103030 (2009)
- [12] P. T. Ernst, S. Götze, J. S. Krauser, K. Pyka, D.-S. Lühmann, D. Pfannkuche, and K. Sengstock, *Nature Phys.* **6**, 56 (2010)
- [13] J. F. Sherson, S. J. Park, P. Pedersen, N. Winter, M. Gajdacz, S. Mai, and J. Arlt, arXiv:1107.1643v1 (2011)
- [14] T. Salger, C. Grossert, S. Kling, and M. Weitz, *Phys. Rev. Lett.* **107**, 240401 (2011)
- [15] G. Wirth, M. Ölschläger and A. Hemmerich, *Nature Phys.* **7**, 147 (2011)
- [16] N. Fabbri, S. D. Huber, D. Clément, L. Fallani, C. Fort, M. Inguscio, and E. Altman, *Phys. Rev. Lett.* **109**, 055301 (2012)
- [17] P. Soltan-Panahi, D.-S. Lühmann, J. Struck, P. Windpassinger, and K. Sengstock, *Nature Phys.* **8**, 71 (2012)
- [18] L. Tarruell, D. Greif, T. Uehlinger, G. Jotzu, and T. Esslinger, *Nature* **483**, 302 (2012)
- [19] J. Heinze, S. Götze, J. S. Krauser, B. Hundt, N. Fläschner, D.-S. Lühmann, C. Becker, and K. Sengstock, *Phys. Rev. Lett.* **107**, 135303 (2011)
- [20] For details see supplemental online material.
- [21] J. Hecker Denschlag, J. E. Simsarian, H. Häffner, C. McKenzie, A. Browaeys, D. Cho, K. Helmerson, S. L. Rolston, and W. D. Phillips, *J. Phys. B: At. Mol. Opt. Phys.* **35**, 3095-3110 (2002)
- [22] T. Stöferle, H. Moritz, C. Schori, M. Köhl, and T. Esslinger, *Phys. Rev. Lett.* **92**, 130403 (2004)
- [23] M. Greiner, I. Bloch, O. Mandel, T. W. Hänsch, and T. Esslinger, *Phys. Rev. Lett.* **87**, 160405 (2001)
- [24] J. S. Krauser, J. Heinze, N. Fläschner, S. Götze, O. Jürgensen, D.-S. Lühmann, C. Becker and K. Sengstock, arXiv:1203.0948v1 (2012)
- [25] C. A. Regal and D. S. Jin, *Phys. Rev. Lett.* **90**, 230404 (2003)
- [26] N. Strohmaier, D. Greif, R. Jördens, L. Tarruell, H. Moritz, T. Esslinger, R. Sensarma, D. Pekker, E. Altman, and E. Demler, *Phys. Rev. Lett.* **104**, 080401 (2010)
- [27] H. Ott, E. de Mirandes, F. Ferlaino, G. Roati, V. Türec, G. Modugno, and M. Inguscio, *Phys. Rev. Lett.* **93**, 120407 (2004)

SUPPLEMENTAL INFORMATION

This supplemental information discusses the preparation of our atomic sample (S1), details of the fitting procedures for the experimental data (S2,S3) and the theoretical calculations both for particle (S4) and hole (S5) excitations.

S1. PREPARATION OF THE ATOMIC SAMPLE

By sympathetic cooling, we create a mixture of spin-polarized ^{87}Rb and ^{40}K atoms in a magnetic trap. The atoms are transferred adiabatically to a crossed optical dipole trap operated at 811 nm with a $1/e^2$ radius of $120\text{ }\mu\text{m}$. After switching off the magnetic trap, we remove the rubidium atoms from the trap using a resonant light pulse. For experiments with spin polarized atoms, the preparation is finished here. For experiments with interacting mixtures, we use a series of rf-pulses and -sweeps to prepare an equal mixture of the hyperfine states $m = -9/2$ and $m = -5/2$ in the hyperfine manifold $f = 9/2$. This mixture is evaporatively cooled in the following by reducing the laser power of the optical dipole trap. The final particle number is about $N = 5 \cdot 10^4$ atoms at typical temperatures of $0.2 T_F$. After the preparation we linearly ramp up an optical lattice within 100 ms. The lattice consists of up to three orthogonal retro-reflected laser beams at $\lambda = 1030\text{ nm}$ with a $1/e^2$ radius of $200\text{ }\mu\text{m}$. For measurements at the Feshbach resonance, the magnetic field was set to the final value 50 ms prior the 100 ms optical lattice ramp.

To initialize the photocurrent, we modulate the amplitude of one of the lattice directions for 1 ms with a frequency, that is resonant with a transition from the lowest energy band to the second excited band. This excites a fraction of particles and leaves vacancies in the lowest band. Due to the different curvature of the bands, the resonance condition depends on the quasimomentum. By tuning the modulation frequency, we have full control over the quasimomentum of the excited particles. Since lattice amplitude modulation does not imprint any quasimomentum, the holes in the lowest energy band have the same quasimomentum as the particles.

S2. ANALYSIS OF EXPERIMENTAL DATA: PARTICLE EXCITATIONS

In this section we describe how we extract the oscillation frequency of the excited atoms from the experimental data. For each time step we determine the quasimomentum of the excitation by taking the center-of-masses of the atoms in the conduction band independently at positive and negative momentum. To be insensitive to global displacements, we measure the difference of both

excitation centers instead of their absolute positions. We extract the oscillation frequencies Ω from the differential center-of-masses by fitting an exponentially damped cosine of the form

$$\Delta q(t) = A \exp(-\Gamma t) \cos(\Omega t + \Phi) + C,$$

with oscillation amplitude A , damping rate Γ , a phase shift Φ and a constant offset C . In the experiment, always two excitations with opposite initial quasimomenta q_0 and $-q_0$ are created. Both excitations independently perform oscillations in the combined potential of lattice and harmonic trap. After a quarter of an oscillation period, both excitations arrive at $q = 0$, are Bragg reflected and continue at the other side of the Brioullin zone, respectively. Since the excitations are not distinguishable, our center of mass determination cannot resolve this. Therefore the extracted data artificially exhibits a turning point of the oscillations at this position. The data thus shows an oscillation with twice the fundamental frequency: $\Omega = 2\omega$. Consequently, the factor of 2 is corrected in all experimental data except for Fig. 1, such that we always show ω instead of Ω .

S3. ANALYSIS OF EXPERIMENTAL DATA: HOLE EXCITATIONS

To determine the depth of the hole excitation in the valence band, we fit a sum of three Gaussians to the first Brioullin zone in the time-of-flight picture. One of the Gaussians represents the atomic background density in the valence band. The other two represent the holes at positive and negative q , respectively. The background is determined from the momentum distribution directly after the excitation for each time series individually. For the dynamical evolution we take the form of the background to be constant for all times and solely allow for a variation of the absolute magnitude as a function of time.

S4. CALCULATION OF CONDUCTION BAND DYNAMICS

In this section we describe the numerical calculations for the particle excitations in the conduction band. To derive quantitative predictions for the oscillations for all initial quasi-momenta, we performed calculations including both the periodic and the harmonic confinement. We assume a single particle confined to the full potential

$$H = \frac{p^2}{2m} + sE_r \cos(k_{BZ}x)^2 + \frac{1}{2}m\omega_0^2x^2.$$

By diagonalizing the homogeneous lattice Hamiltonian $H_0 = p^2/2m + sE_r \cos(k_{BZ}x)^2$ for a single particle, we

obtain the Bloch states for a given lattice depth s . In energy space, the system has bands of allowed states divided by gaps where no states are located. In the experiment, the initial excitation is produced by a lattice amplitude modulation pulse of $t = 1$ ms duration. This pulse width is much larger than the trapping frequency ω_0 . For the parameters discussed here, it holds in general, that

$$E_C \gg \hbar/t \gg \hbar\omega_0,$$

where E_C is the band width of the conduction band. Therefore, the harmonic confinement is negligible during the preparation. In all calculations we assume a distribution of Bloch states centered at a certain quasi-momentum q_0 . For simplicity we use a Gaussian distribution, with a variance $\sigma = 364.5$ Hz, corresponding to the width of the 1 ms lattice modulation. We obtain the time evolution by exact diagonalization of the full Hamiltonian H which leads to a non-trivial dynamics as shown in Fig. 3(b). To extract the oscillation frequencies from the dynamics, we calculate the center-of-mass of the quasi-momentum distribution with respect to the homogeneous lattice Hamiltonian H_0 and fit a cosine to the data. For a typical calculation we use up to 400 quasi-momenta and 11 bands.

In the calculations we only use one excitation which has a positive quasi-momentum. We clearly observe the Bragg reflection at $q = 0$ and obtain an oscillation frequency in agreement with the approximation of equation (1). As mentioned in section S2, the analysis of

the experimental data results in twice the oscillation frequency, since excitations at positive and negative quasi-momentum are indistinguishable. This effect is consistently reproduced by the calculations, if we incoherently overlap two excitations with opposite sign in the quasi-momentum, as shown in Fig. 3(b).

S5. CALCULATION OF HOLE DYNAMICS

For electron gases in solids a missing electron can be described as a single particle with negative mass. Such a hole is in complete analogy to an electron. We adopted this prescription for holes in the valence band of our harmonically trapped quantum gas. To describe this situation numerically, we assumed a single particle with negative mass $m^* = -m$ in the valence band and calculated its evolution in the presence of the harmonic confinement and the lattice potential. The excitation has the same shape as in the conduction band, since the missing atoms in the valence band directly correspond to excited atoms in the conduction band. We also take into account the finite filling of the valence band. This is done by using only the lowest energy states in the time evolution of the initial state. Finally, we include finite temperature by using a Fermi-Dirac distribution instead of a sharp edge when weighting the included eigenstates of H . To match the occupation number to the experimental situation, we take the total atom number and the trapping frequencies and calculate the number of occupied states in the appropriate direction.